Impact of Land Surface Models on Simulation of Extreme Rainfall Events over Upper Catchments of The River Indus

Sultan, S.[1, 2], L. Hui[3, 4], M. Riaz[2], Z. A. Babar[2], W. Renguang[5],
I. Ahmad[2], I. Ahmad[6], M. A. Shad[2], C. M. Aslam[2]

Abstract

Water management in arid and sub-arid regions is critical and it could turn out to be precarious over the mountainous regions like Upper Indus basin due to related hazards; flash flooding, debris flow, land sliding, etc. The WRF-ARW (v5.3.1) modelling framework is coupled with Unified Noah and Noah-MP land surface models (LSM) with various physical schemes and domain setup. This setup helps to investigate the impact of LSM physics on rainfall simulation over the upper Indus basin and their possible links with landuse datasets. We use GIS platform to modify and rectify the landuse datasets to investigate the impact on rainfall simulations with different physical parameterizations in WRF modelling setup. In nested domain, all simulations coupled with Noah-MP shows negative bias (i.e. overestimation) for rainfall over the mountain areas, while there is no significant impact on storm structure when the single domain is considered for both unified Noah and Noah-MP LSM. Furthermore, Noah-MP improves the rainfall simulations over the complex terrain, and there is no substantial impact in the plains of River Indus. Moreover, updated landuse and corrected elevation dataset also slightly improves the simulation quality and MODIS landuse shows marginally negative bias in urban areas as compared to default USGS landuse dataset.

Key Words: rainfall, WRF, landuse models, GIS, complex terrain, Pakistan

Introduction

The 20th century was witnessed as the wettest period over the past millennium (Treydte et al. 2006; Sun et al. 2006; Rehman et al. 2012; Hanif et al. 2013; Palazzi et al. 2013). The same observation holds for many parts of the world. For example, the study done (Goswami et al. 2006; Rajeevan et al. 2008) in India, in China (Zhai et al. 2005; Miao et al. 2011), in South Portugal (Costa & Soares 2009), in United Kingdom (Fowler & Kilsby 2003), etc. Similarly, these rainfall trends are likely to continue with more severity in most parts of the world (IPCC 2013).

The sensitivity of simulated rainfall depends on various physical schemes, including microphysics, planetary boundary layer, cumulus, etc. Moreover, it also depends on the land surface model's physics (Chang et al. 2009, Kang et al 2014), which is responsible for resolving the interactions between land processes and atmosphere (Noilhan & Planton 1989). Land surface models (LSMs) simulate the surface fluxes in response to feedback from the near surface atmospheric forcing (e.g. soil moisture, soil temperature, snow, vegetation, water vapour, momentum, CO_2, etc.). These processes have pronounced influences on atmospheric boundary layer (Liu et al. 2007; Ek et al. 2003). Therefore, sensitivity and impact analysis of LSMs parameterization is important when considering rainfall simulation over the complex terrain.

In most studies Noah-MP (Niu et al. 2011; Yang et al. 2011) is not coupled with WRF core to analyse the land surface interaction with updated static and parameterization schemes. Most of the studies ignore that Noah-MP land surface models are more sensitive to static data and initial condition as compared to relatively simple land surface models, e.g., RUC (Benjamin & Grell 2004) and unified Noah (Tewari et al. 2004).

[1] shahzad.sultan@gmail.com
[2] Pakistan Meteorological Department, Flood Forecasting Division, Lahore.
[3] Institute of Space and Earth Information Science, Chinese University of Hong Kong, Hong Kong.
[4] Department of Geography and Resource Management, Chinese University of Hong Kong, Hong Kong.
[5] Institute of atmospheric physics Chinese Academy of Sciences, Beijing, China.
[6] Department of Geography, University of Baluchistan, Pakistan.

The advances in Weather Research and Forecasting (WRF) modelling system and enhancement of computational power during last few years are remarkable (see figure 2 for schematic diagram of WRF modelling framework). Now we have more flexible and portable modelling framework, numerous forcing and boundary conditions, more sophisticated and multiple physical schemes, up-to-date landuse and other terrain related datasets (elevation, aerosol, vegetation, etc.). Similarly, wider range of compatibility options of WRF with multiple datasets and other modelling systems tremendously increase the research horizon and its capabilities (Shamarock et al. 2008; Michalakes et al. 2004; Maussion et al. 2010; Stensrud 2007; Sun et al. 2006).

Data and Methodology

GFS0.5 gridded data (Unidata et al. 2003) produced by National Centres for Environmental Prediction (NCEP) is used as forcing and lateral boundary conditions. We use two kinds of datasets – rain gauged and TRMM – to compare the simulated results. Rain gauged and TRMM data is shown in Table 1 for 45 locations, which is provided by Pakistan Meteorological Department, and Figure 1 shows their geographical locations.

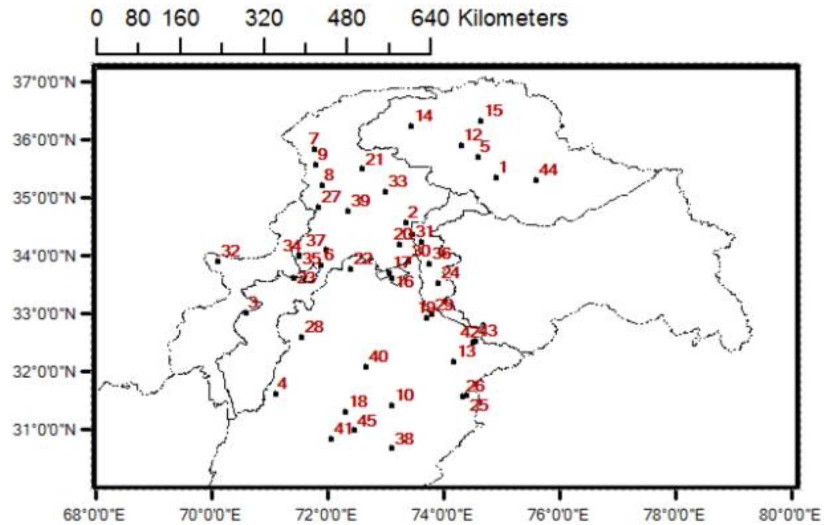

Figure 1: Study Area and Observatories Location donated by their serial number as given in Table 1. Serial numbers are used to understand the spatial variability and distribution of simulated rainfall. E.g., the serial number 40, 10, 18, 45, 41, 38, 26 and 25 lies over the Indus Plains (so-called central zone) while 14, 15, 12, 5, 1 and 44 lies in extreme north part of study area (so called north zone)

Numerous simulations with different physical parameters and spin-up times are run to optimise the model for extreme rainfall event of 26-30 July 2010, which was initiated at 25 July 2010 00:00, and tested with various combinations. Readers are advised to consult Ullah & Shouting (2013) & Webster et al. (2011) to get the detailed synoptic characteristics of this rainfall event. Here we coupled new LSM, Noah-MP to WRF modelling setup, which is recently introduced to WRF modelling setup and has not comprehensively evaluated. Similarly, unified updated Noah land surface model is also coupled for comparative study. This sensitivity and the qualitative comparison are performed with various other physical schemes and static datasets as shown in Table 2.

Table 1: Meteorological observatories, their elevations and accumulated rainfall during 26-30 July 2010.

Sr.	Name	Lat.	Long.	Elev.	Observed	TRMM
1	ASTORE	35.33	74.9	3771	37	37
2	BALAKOT	34.55	73.35	1011	251	240
3	BANNU	33	70.6	388	92	109
4	BHAKKAR	31.6	71.1	169	35	41
5	BUNJI	35.7	74.6	1485	8	21

6	CHERAT	33.82	71.89	1216	372	355
7	CHITRAL	35.83	71.78	1448	60	61
8	DIR	35.2	71.9	1642	301	252
9	DROSH	35.55	71.8	1546	99	118
10	FAISALABAD	31.4	73.1	187	16	19
11	GARHI_DOPATTA	34.23	73.61	848	31	180
12	GILGIT_PBO	35.9	74.3	2183	30	32
13	GUJRANWALA	32.15	74.18	225	10	27
14	GUPIS	36.23	73.44	2188	54	64
15	HUNZA	36.31	74.65	2057	36	37
16	ISLAMABAD_AP	33.6	73.1	502	220	218
17	ISLAMABAD_ZP	33.69	73.06	534	208	221
18	JHANG	31.3	72.3	152	19	22
19	JHELUM	32.92	73.72	225	45	67
20	KAKUL_ABBOTTABAD	34.18	73.25	1222	191	219
21	KALAM	35.48	72.59	1980	132	155
22	KAMRA	33.75	72.4	316	312	311
23	KOHAT	33.6	71.43	530	294	293
24	KOTLI	33.52	73.9	605	211	173
25	LAHORE_AP	31.58	74.4	217	1	3
26	LAHORE_PBO	31.55	74.33	213	0	2
27	LOWER_DIR	34.82	71.84	747	269	272
28	MIANWALA	32.58	71.55	210	221	221
29	MAND_BAHAUDDIN	32.97	73.8	229	64	66
30	MURREE	33.9	73.4	1895	373	238
31	MUZAFFARABAD	34.36	73.47	694	291	226
32	PARACHINAR_PBO	33.9	70.1	1744	65	82
33	PATTAN_KOHISTAN	35.1	73	914	234	231
34	PESHAWAR_AP	33.99	71.52	362	334	287
35	PESHAWAR_CITY	34	71.5	362	226	286
36	RAWALAKOT	33.85	73.75	1602	11.1	57
37	RISALPUT	34.08	71.97	315	415	389
38	SAHIWAL	30.66	73.11	175	30	30
39	SAIDU_SHARIF	34.75	72.35	963	338	318
40	SARGODHA	32.07	72.67	192	40	42
41	SHORKOT	30.83	72.07	166	28	30
42	SIALKOT	32.5	74.5	249	88	85
43	SIALKOT_AP	32.51	74.56	251	94	87
44	SKARDU_PBO	35.3	75.6	2234	3	7
45	TT_SINGH	30.97	72.47	163	60	48

Table 2: Physical schemes combinations to evaluate the Noah and Noah-MP land surface model impact on rainfall simulation; MP refers to microphysics scheme, SWR refers to shortwave radiation schemes and LWR refers to Long wave radiation scheme,

Simulation	Landuse	MP	PBL	Cumu-lus	LSM	Surface Layer	SWR	LWR
LA_L2	USGS	WSM6	YSU	KF	Noah	MM5	CAM	CAM
LA_L4	USGS	WSM6	YSU	KF	Noah-MP	MM5	CAM	CAM
LB_L2	USGS	CAM	YSU	KF	Noah	MM5	CAM	CAM
LB_L4	USGS	CAM	YSU	KF	Noah-MP	MM5	CAM	CAM
LC_L2	MODIS30s	WSM6	YSU	GD	Noah	Rev.MM5	CAM	CAM
LC_L4	MODIS30s	WSM6	YSU	GD	Noah-MP	Rev.MM5	CAM	CAM
LD_FB0_L2	USGS	WSM6	YSU	KF	Noah	Rev.MM5	CAM	CAM

LD_FB0_L4	USGS	WSM6	YSU	KF	Noah-MP	Rev.MM5	CAM	CAM
LE_L2	MODIS15s	WSM6	UW	ZMF	Noah	Eta	CAM	CAM
LE_L4	MODIS15s	WSM6	UW	ZMF	Noah-MP	Eta	CAM	CAM
LF_L2_Single	USGS	WSM6	YSU	---	Noah	MM5	CAM	CAM
LF_L4_Single	USGS	WSM6	YSU	---	Noah-MP	MM5	CAM	CAM
LG_L2	MODIS30s	WSM6	YSU	BMJ	Noah	MM5	Dudhia	RRTM
LG_L4	MODIS30s	WSM6	YSU	BMJ	Noah-MP	MM5	Dudhia	RRTM

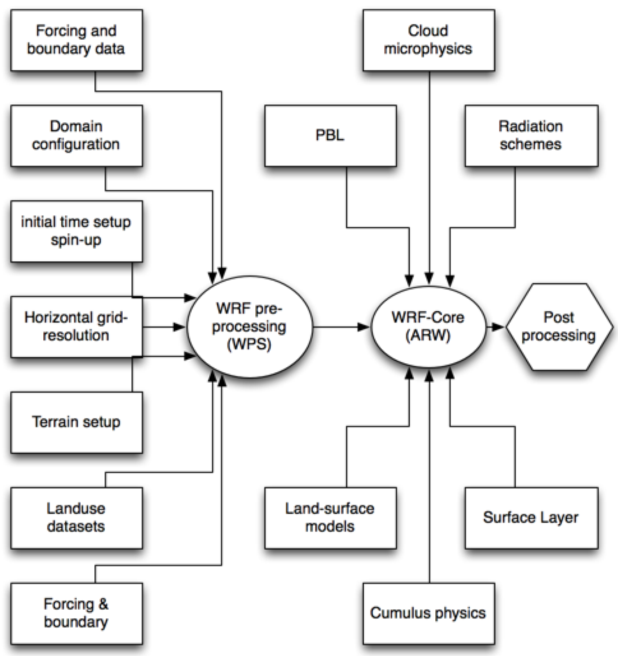

Figure 2: Schematic diagram for WRF, system: Skamarock et al. (2008).

Model Description and Configuration

Weather Research and Forecasting Model (W, sourceRF-ARWv5.3.1) is the next generation distributed mesoscale Numerical Weather Prediction (NWP) Model. It was developed by the combined effort of number of institutes, including, National Centre for Atmospheric Research's (NCAR), the National Oceanic and Atmospheric Administration's (NOAA), National Centres for Environmental Prediction (NCEP) and Earth System Research Laboratory (ESRL) etc. (Skamarock, et al., 2008). It allows parallel computation with a wide range of coupling capabilities to meet the trends of multi-scale multi-model simulations (Michalakes, et al., 2004). This setup also helps scientists to address the challenges of integrating the different atmospheric spheres, including hydrosphere, atmosphere and anthrosphere, which widen its application horizon (Michalakes J., 2010).

24-hour spin-up time is selected for most of the simulations but not limited to this. We have also employed 12 and 36 hours as spin-up time and found that 24 hours is the most optimum. The standard domain setup is shown in Figure 3, which consists of grid spacing of 50 km for parent and 3.3 km for a most inner domain with grid ratio 1:3:5. The grid ratio represents the nesting setup in connection with parent domain, i.e., parent domain has 50 km horizontal grid spacing, so the second domain will be one-third of parent domain (16.5) and the most inner domain will be one-fifth of second domain (3.3 km). Model is set for 28 vertical levels with 50hpa pressure at the top. The domain 2 covers Pakistan including North and western India, part of eastern Iran and Afghanistan regions, while, the most inner domain covered the North of Pakistan and cantered at 33.74 N and 74.1 E.

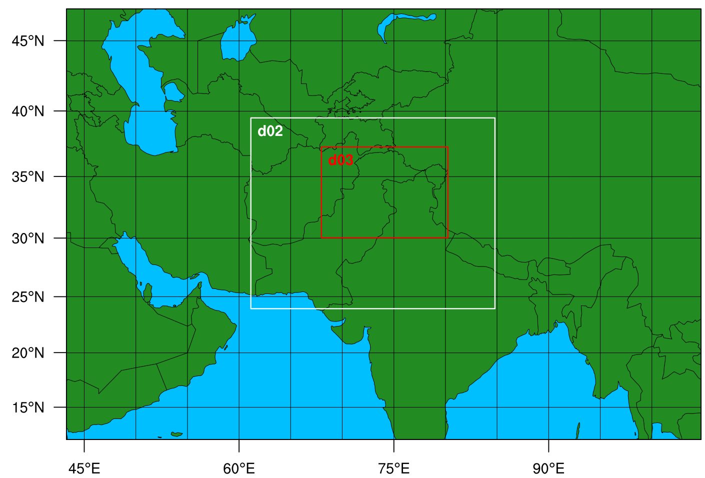

Figure 3: Domain Configuration

We employed WRF Single–moment 6–class (WSM6) (Hong & Lim 2006) and CAM V5.1 2–moment 5–class (CAM) (Eaton 2011) microphysics schemes. Similarly, Updated Yonsei University (YSU) (Hong et al. 2006) and University of Washington TKE (UW) (Bretherton & Park 2009) planetary boundary layer schemes are considered. For cumulus schemes, we use Kain–Fritsch (KF) (Kain 2004), Zhang–McFarlane (ZMF) (Zhang & McFarlane 1995) and Betts–Miller–Janjic (BMJ) (Janjić & Janjic 1994). MM5 Similarity (MM5) (Paulson 1970), (Dyer & Hicks 1970), Revised MM5 (Jiménez et al., 2012) and Eta Similarity (Janjic 2002) surface layer schemes are employed, and for radiation schemes we use CAM longwave and shortwave (Collins et al. 2004), Dudhia shortwave (Dudhia 1989) and RRTM longwave (Mlawer et al. 1997), as mentioned in Table 2.

The grid resolution of less than 5 km may not need cumulus parameterization, but the coarser grid resolution, i.e. more than 10 km may need cumulus parameterization to resolve the convective processes within the grid. Therefore, we did not use cumulus schemes for the most inner domain that has 3.3 km grid resolution, but cumulus schemes are applied to the parent and second domains that have 50 and 16.5 km grid resolution respectively. It is also worth to mention that the spatial grid resolution between 5 and 10 km is not recommended for convective rainfall simulation to avoid the potential errors due to model constraints in resolving convective system. Furthermore, cumulus schemes are bound with PBL schemes and PBL schemes selection is also sensitive to horizontal grid resolution (Aligo et al. 2009).

Since WRF-ARW uses obsolete Landuse Landover (LULC) data from USGS (Loveland & Reed 2000) as default, which was prepared from the Advanced Very High-Resolution Radiometer (AVHRR) instrument using 1992-1993 data, having about 1 km spatial resolution. Furthermore, one can also use MODIS IGBP (International Geosphere-Biosphere Programme) landuse data, which have 1 km to 500m spatial resolution and based on 2001–2006 dataset (Friedl et al. 2002; Belward et al. 1999). Similarly, we have also incorporated SRTM 90m terrain data along with default USGS 1 km. These datasets are modified using GIS platform, and compatibility has been made using modified Fortran coding, originally provided by ARW Version 3 Modelling System User's Guide (Wang et al. 2014).

Results and Discussion

The updated terrain datasets marginally increase the model performance and show more sensitivity when simulated with complex physical schemes. Furthermore, MODIS30s and MODIS15s landuse slightly increase the rainfall amount in the urban areas of north-west and central zones, but there is no significant impact in north and northeast zones. Similarly, MODIS15s and default USGS30s do not differ much when considered the accumulative impact on rainfall but MODIS30s shows more sensitivity when compared with default landuse data. This is because of the better representation of urban areas in new landuse datasets, which increases the radiation fluxes and also causes a slight increase in temperature.

Mostly, Noah LSM fails to capture the storm structure in all simulations except single domain (see simulation LF and graph for simulation LF) and nested domain without feedback (see simulation LD and its graph). This is possibly due to the impact of cumulus scheme, which was only used in nested domain setup but further investigation is needed to understand this behaviour of unified Noah LSM for single domain setup and a possible link with cumulus parametrization. However, rainfall showed eastward shift in the north and north-west zones, when simulated with Noah LSM, see simulations LA_L2 and LD_FB0_L2 (Here FB0 refers to zero feedback, i.e. without feedback). Furthermore, CAM microphysics failed to simulate the storm structure and shows positive bias (less rain) both with Noah and Noah-MP LSMs.

Table 3: Correlation and RMSE for Noah and Noah-MP land surface models

Simulation	Correlation	RMSE
LA_L2	0.22	153
LA_L4	0.72	105
LB_L2	0.35	159
LB_L4	0.69	140
LC_L2	0.54	137
LC_L4	0.45	139
LD_FB0_L2	0.47	124
LD_FB0_L4	0.67	100
LE_L2	0.55	134
LE_L4	0.62	137
LF_L2_Single	0.30	130
LF_L4_Single	0.53	111

Table 3 depicts that the simulations run with Noah-MP has stronger correlation and less root mean square error as compared to unified Noah LSM when matched with observed data. The strongest correlation, i.e. 0.72 exists when Noah-MP is coupled with WRF-core with combinations, as mentioned in Table 3 in simulation LA_L4, while the weakest correlation is 0.22 (see simulation LA_L2). Simulations LC, LE and LG has common rainfall distribution, which shows a positive bias in the north and negative bias over the plains of River Indus, and do not simulate the rainfall pattern by observed rainfall distribution. It needs to be remembered that these three simulations do not use KF cumulus scheme. Therefore, it is concluded that KF is the most reliable cumulus parametrization in our simulation experiments.

Comparison of observed and simulated rainfall is shown from Figure ‘a’ to Figure ‘f’. Overall, simulations LB, LC and LE shows a positive bias, while figure d and figure f shows that both Noah and Noah-MP exhibits close to each other, this is also mentioned and discussed in the previous paragraph. It is further described that the y-axis is the rainfall in mm in the figures given below.

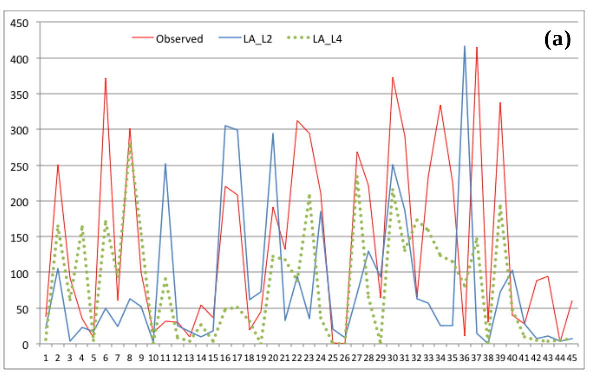

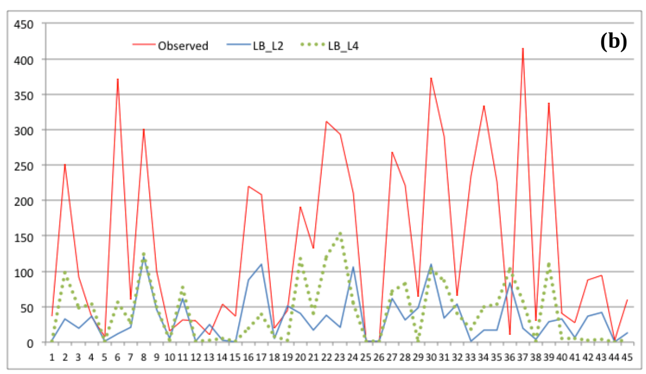

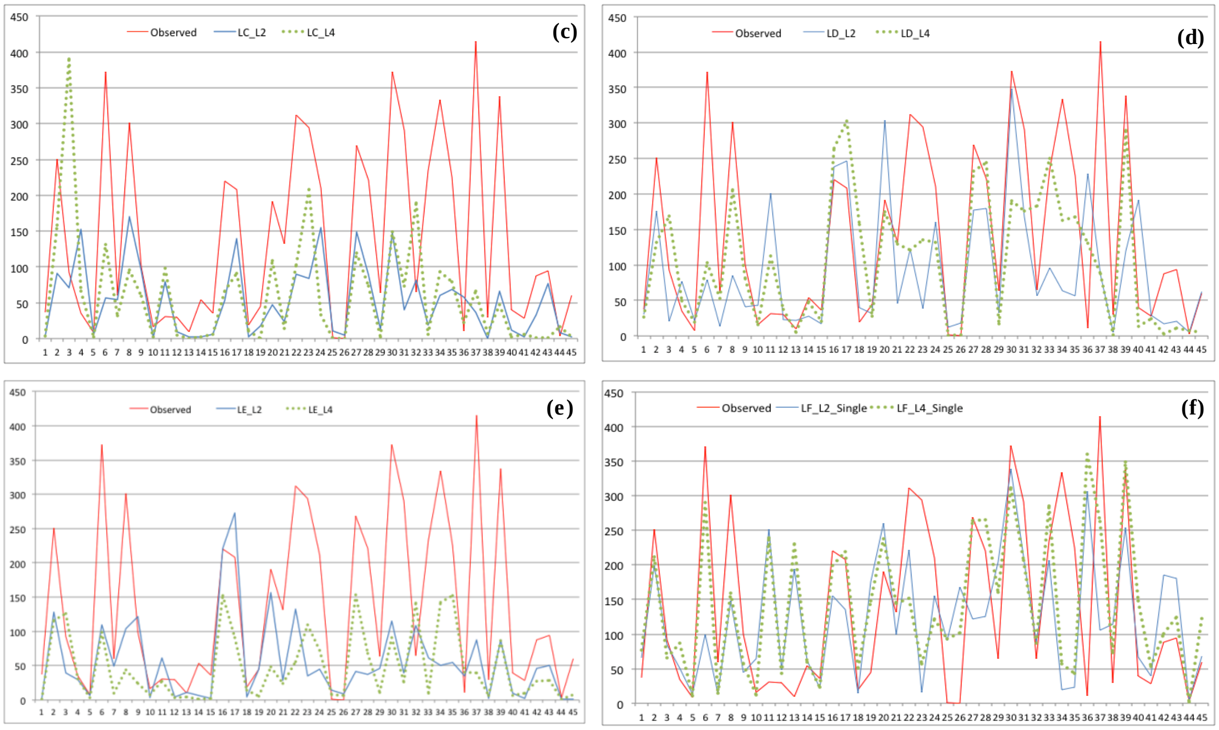

Simulation results for Noah and Noah-MP land surface models with various physical schemes

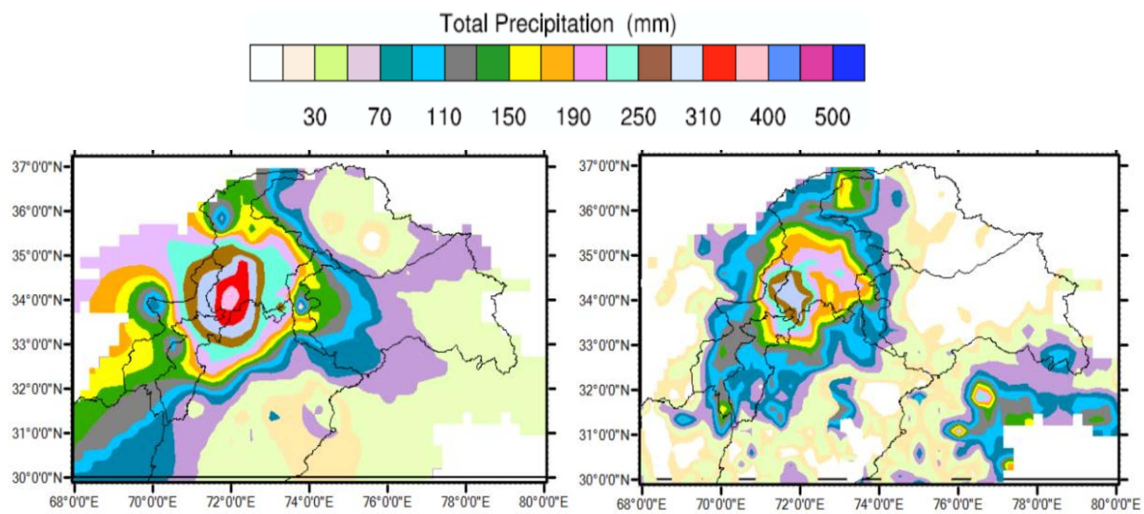

Interpolated observed rainfall from 45 meteorological stations

TRMM rainfall distribution

LA_L2 LA_L4 LB_L2 LB_L4

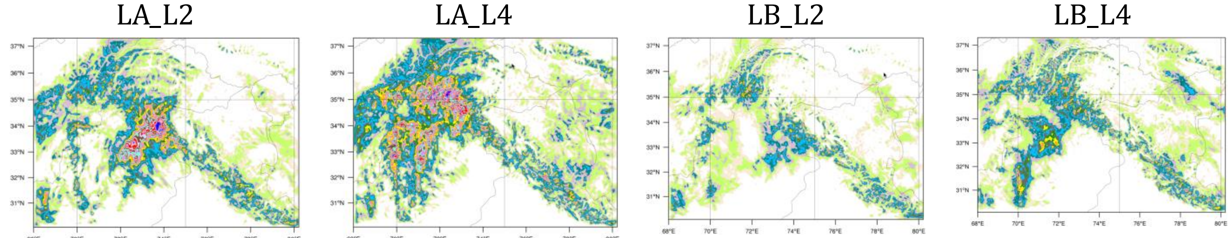

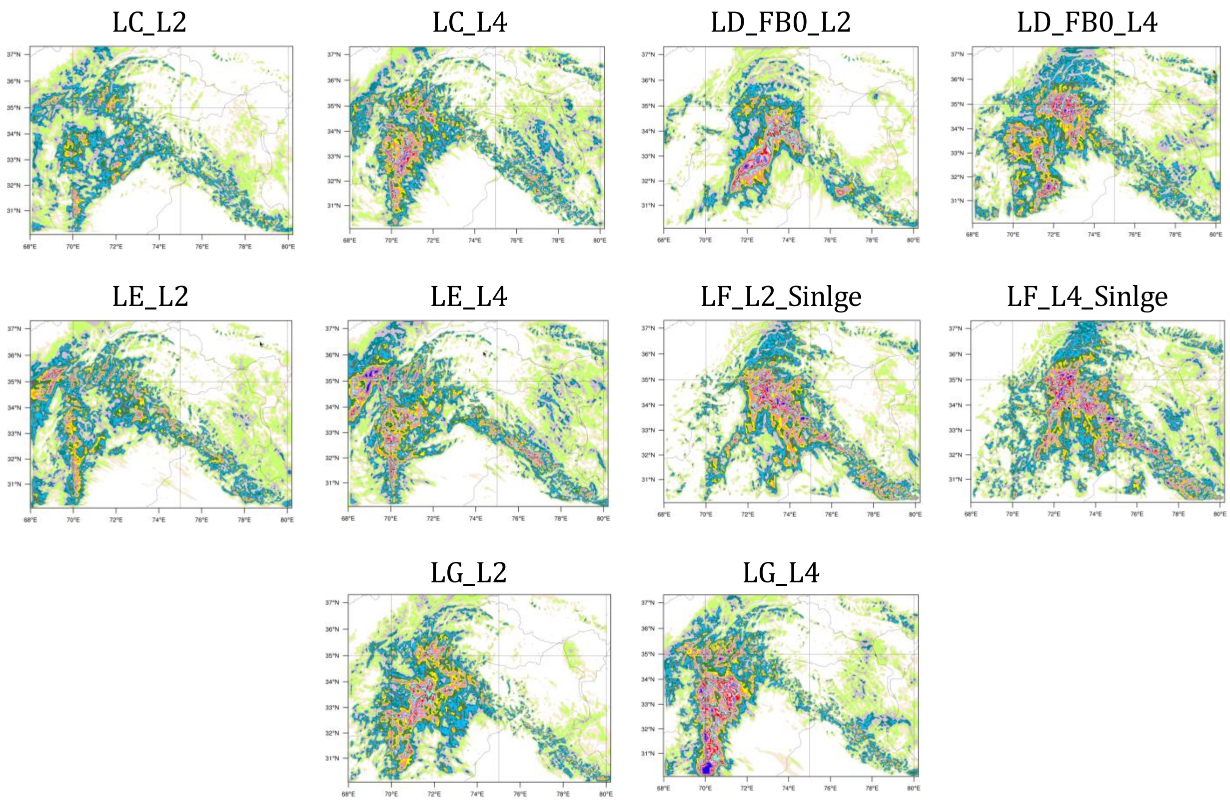

Conclusion

It is concluded that Noah LSM performs better over flat terrain when simulated with YSU PBL scheme during the post monsoon period. While, Noah-MP shows better agreement with observed rainfall over complex as well as flat terrain when simulated with ACM2 PBL scheme. Similarly, rainfall significantly overestimated when used Noah-MP with YSU PBL scheme. Furthermore, the classic structure of rainfall event-A i.e. split into two cells is well captured by Noah-MP in nested domain setup but failed in single domain or domain without feedback. All simulations coupled with Noah-MP increases the rainfall amount significantly, while there is no significant impact on storm structure when we take single domain. Therefore, generally land surface model behaves differently with seasonal shift and terrain features. These variations are possibly due to changes in land surface processes associated with seasonal change and have static (fixed) corresponding parameters in model setup. Furthermore, Noah LSM fails to capture the storm structure in most of the simulations, and produce an eastward shift of rainfall. There is a slight improvement with Noah LSM when coupled with the single domain or one-way nested domain setup.

References

Aligo, E. A., W. A. Gallus, & M. Segal, 2009: On the Impact of WRF Model Vertical Grid Resolution on Midwest Summer Rainfall Forecasts. Weather and Forecasting, 24(2), pp.575–594.

Belward, A. S., J. E. Estes, & K. D Kline, 1999: The IGBP-DIS Global 1-Km Land-Cover Data Set DISCover: A Project Overview. Photogrammetric Engineering and Remote Sensing, 65(9), pp.1013–1020.

Benjamin, S., & G. Grell, 2004: Mesoscale weather prediction with the RUC hybrid isentropic-terrain-following coordinate model. Monthly Weather

Bretherton, C. S. & S. Park, 2009: A New Moist Turbulence Parameterization in the Community Atmosphere Model. Journal of Climate, 22(12), pp.3422–3448.

Chang, H. I. et al., 2009: The role of land surface processes on the mesoscale simulation of the July 26, 2005 heavy rain event over Mumbai, India. Global and Planetary Change, 67(1–2), pp.87–103.

Collins, W. D. et al., 2004: Description of the NCAR community atmosphere model (CAM 3.0).

Costa, A. C. & A. Soares, 2009: Trends in extreme precipitation indices derived from a daily rainfall database for the South of Portugal. International Journal of Climatology, 29(13), pp.1956–1975.

Dudhia, J., 1989: Numerical Study of Convection Observed during the Winter Monsoon Experiment Using a Mesoscale Two-Dimensional Model. Journal of the Atmospheric Sciences, 46(20), pp.3077–3107.

Dyer, A. J., & B. B. Hicks, 1970: Flux-gradient relationships in the constant flux layer. Quarterly Journal of the Royal Meteorological Society, 96(410), pp.715–721.

Eaton, B., 2011: User's Guide to the Community Atmosphere Model CAM-5.1,

Ek, M. B. M. et al., 2003: Implementation of Noah land surface model advances in the National Centers for Environmental Prediction operational mesoscale Eta model. Journal of Geophysical Research, 108(D22), p.8851.

Fowler, H. J., & C. G. Kilsby, 2003: A regional frequency analysis of United Kingdom extreme rainfall from 1961 to 2000. International Journal of Climatology, 23(11), pp.1313–1334.

Friedl, M., D. McIver, & J. Hodges, 2002: Global land cover mapping from MODIS: algorithms and early results. Remote Sensing of ….

Goswami, B. N. et al., 2006: Increasing trend of extreme rain events over India in a warming environment. Science (New York, N.Y.), 314(5804), pp.1442–5.

Hanif, M., A. H. Khan, & S. Adnan, 2013: Latitudinal precipitation characteristics and trends in Pakistan. Journal of Hydrology, 492, pp.266–272.

Hong, S. Y., & J. O. J. Lim, 2006: The WRF single-moment 6-class microphysics scheme (WSM6). J. Korean Meteor. Soc, 42(2), pp.129–151.

Hong, S. Y., Y. Noh, & J. Dudhia, 2006: A New Vertical Diffusion Package with an Explicit Treatment of Entrainment Processes. Monthly Weather Review, 134(9), pp.2318–2341.

IPCC, 2013. Summary for Policymakers. In T. F. Stocker et al., eds. Climate Change 2013: The Physical Science Basis. Contribution of Working Group I to the Fifth Assessment Report of the Intergovernmental Panel on Climate Change. Cambridge, United Kingdom and New York, NY, USA: Cambridge University Press, pp. 1–30.

Janjic, Z., 2002: Nonsingular Implementation of the Mellor-Yamada Level 2.5 Scheme in the NCEP Meso model. NCEP Office Note, 437, p.61.

Janjić, Z. I., 1994: The Step-Mountain Eta Coordinate Model: Further Developments of the Convection, Viscous Sublayer, and Turbulence Closure Schemes. Monthly Weather Review, 122(5), pp.927–945.

Jiménez, P. P. A. et al., 2012: A revised scheme for the WRF surface layer formulation. Monthly Weather Review, 140(3), pp.898–918.

Kain, J. J. S., 2004: The Kain-Fritsch convective parameterization: an update. Journal of Applied Meteorology, 43(1), pp.170–181.

Kang, S., E. S. S. Im, & J. B. B. Ahn, 2014: The impact of two land-surface schemes on the characteristics of summer precipitation over East Asia from the RegCM4 simulations. International Journal of Climatology, 34(15), pp.3986–3997.

Liu, S. et al., 2007: Numerical simulations of land surface physical processes and land-atmosphere interactions over oasis-desert/Gobi region. Science in China Series D: Earth Sciences, 50(2), pp.290–295.

Loveland, T. & B. Reed, 2000: Development of a global land cover characteristics database and IGBP DISCover from 1 km AVHRR data. … Journal of Remote ….

Maussion, F. et al., 2010: WRF simulation of a precipitation event over the Tibetan Plateau, China-an assessment using remote sensing and ground observations. Hydrology and Earth System Sciences Discussions, 7(6), pp.3551–3589.

Miao, S. et al., 2011: Impacts of Urban Processes and Urbanization on Summer Precipitation: A Case Study of Heavy Rainfall in Beijing on 1 August 2006. Journal of Applied Meteorology and Climatology, 50(4), pp.806–825.

Michalakes, J. et al., 2004: The Weather Research and Forecast Model: Software Architecture and Performance. Use of High Performance Computing in Meteorology Proceedings of the Eleventh ECMWF Workshop, (June), pp.156–168.

Mlawer, E. J. et al., 1997: Radiative transfer for inhomogeneous atmospheres: RRTM, a validated correlated-k model for the long wave (Paper 97JD00237). JOURNAL OF GEOPHYSICAL RESEARCH-ALL SERIES-, 102, pp.16–663.

Niu, G. et al., 2011: The community Noah land surface model with multiparameterization options (Noah-MP): 1. Model description and evaluation with local-scale measurements. Journal of Geophysical Research: Atmospheres (1984–2012), 116(D12).

Noilhan, J., & S. Planton, 1989: A Simple Parameterization of Land Surface Processes for Meteorological Models. Monthly Weather Review, 117(3), pp.536–549.

Palazzi, E., J. Hardenberg, & A. Provenzale, 2013: Precipitation in the Hindu-Kush Karakoram Himalaya: Observations and future scenarios. Journal of Geophysical Research: Atmospheres, 118(1), pp.85–100.

Paulson, C.A., 1970: The mathematical representation of wind speed and temperature profiles in the unstable atmospheric surface layer. Journal of Applied Meteorology, 9(6), pp.857–861.

Rajeevan, M., J. Bhate, & A. K. Jaswal, 2008: Analysis of variability and trends of extreme rainfall events over India using 104 years of gridded daily rainfall data. Geophysical Research Letters, 35(18), p.L18707.

Rehman, S., M. A. Shah, & S. Salma, 2012: Rainfall trends in different climate zones of Pakistan. Pakistan Journal of Meteorology (Pakistan), 9(17), pp.37–47.

Shamarock, W. et al., 2008: A description of the advanced research WRF version 3. NCAR technical note NCAR/ …, 113(June).

Skamarock, W. C. et al., 2008: A Description of the Advanced Research WRF Version 3. Technical Report, (June), p.113.

Stensrud, D., 2007: Parameterization schemes: keys to understanding numerical weather prediction models, Cambridge University Press.

Sun, Y. et al., 2006: How Often Does It Rain? Journal of Climate, 19(6), pp.916–934.

Tewari, M. et al., 2004: Implementation and verification of the unified NOAH land surface model in the WRF model. In 20th conference on weather analysis and forecasting/16th conference on numerical weather prediction. pp. 11–15.

Treydte, K.S. et al., 2006: The twentieth century was the wettest period in northern Pakistan over the past millennium. Nature, 440(7088), pp.1179–82.

Ullah, K. & G. Shouting, 2013: A diagnostic study of convective environment leading to heavy rainfall during the summer monsoon 2010 over Pakistan. Atmospheric Research, 120–121, pp.226–239.

Webster, P.J., V. E. Toma, & H. M. Kim, 2011: Were the 2010 Pakistan floods predictable? Geophysical Research Letters, 38(4), p.n/a-n/a.

Wei Wang, C. B. M .D. J. D. D. G. H. L., 2014: ARW Version 3 Modelling System User's Guide.

Yang, Z. Z. L. Z. et al., 2011: The community Noah land surface model with multiparameterization options (Noah-MP): 2. Evaluation over global river basins. Journal of Geophysical Research: Atmospheres (1984–2012), 116(D12), p.D12110.

Zhai, P. et al., 2005: Trends in Total Precipitation and Frequency of Daily Precipitation Extremes over China. Journal of Climate, 18(7), pp.1096–1108.

Zhang, G. J. & N. A. McFarlane, 1995: Sensitivity of climate simulations to the parameterization of cumulus convection in the Canadian climate centre general circulation model. Atmosphere-Ocean, 33(3), pp.407–446.